Polymer 77 (2015) 10–13

Contents lists available at ScienceDirect

Polymer

journal homepage: www.elsevier.com/locate/polymer

Short communication

Interfacial dynamics of polydimethylsiloxane adsorbed on fumed metal oxide particles of a wide range of specific surface area

Panagiotis Klonos*, Apostolos Kyritsis, Polycarpos Pissis

Department of Physics, National Technical University of Athens, Zografou Campus, 15780 Athens, Greece

ARTICLE INFO

Article history:
Received 5 June 2015
Received in revised form
5 September 2015
Accepted 8 September 2015
Available online 11 September 2015

Keywords:
Glass transition
Interfacial relaxation
Dielectric spectroscopy

ABSTRACT

Interfacial dynamics of polydimethylsiloxane adsorbed on silica and titania nanoparticles of a wide range of specific surface area (S, 25–342 m^2/g) and size (8–80 nm in diameter for primary particles) was studied employing differential scanning calorimetry (DSC) and broadband dielectric spectroscopy (BDS). Both techniques revealed an increase of the interfacial polymer fraction with increasing of surface roughness S, accompanied with an enhancement of dynamics and cooperativity of the corresponding segmental relaxation (interfacial relaxation, α_{int}). At the same time, bulk dynamics (glass transition temperature, T_g, and time scale of α relaxation) was not significantly affected. The results are discussed in terms of bimodal conformations of polymers adsorbed on solid surfaces and in terms of an increase of the apparent thickness of the interfacial layer with increasing of surface roughness.

The existence of an *interfacial polymer fraction* in polymer nanocomposites (PNCs) [1–4], characterized by a modified structure [5–7], slower dynamics [2,8–11] and increased thermal stability [12], as compared to the bulk, has been found to affect significantly or even dominate the properties of PNCs [3,13]. Pissis and coworkers suggested that the stronger polymer–particle hydrogen bonding is at the origin of the increased interfacial layer thickness in polydimethylsiloxane (PDMS)/titania as compared to PDMS/silica conventional PNCs [2,8]. Kumar and coworkers suggested that the interfacial layer thickness may decrease with curvature of the adsorbing surface [14] and increase with size of nanoparticles [15].

We have recently demonstrated similarities in the behavior of linear PDMS adsorbed on fumed silica particles in *core–shell* type PNCs [11] with that of polymers adsorbed on flat solid surfaces [16–18] and in conventional PNCs [8–10]. The surface and porosity characteristics of fumed silicas are reflected in the specific surface area, S [9,11,19]. An interesting question, so far not considered in the literature, refers to the dependence of the characteristics of the interfacial polymer fraction on S.

In the present study, results by differential scanning calorimetry (DSC) and broadband dielectric relaxation spectroscopy (BDS) in systems based on linear PDMS (*MW* ~ 7960, degree of polymerization ~105 monomers/chain, $-CH_3$ terminated, Kremniypolymer, Zaporozhye, Ukraine) (40 wt%) adsorbed (via hydrogen bonding [2]) on aggregates of fumed metal oxide particles of a wide range of S, are discussed in terms of dynamics in the interfacial layer and evaluation of the interfacial polymer fraction and apparent thickness of the interfacial layer. The metal oxides used are titania (~70 nm in diameter for primary particles, ~800 nm in size for aggregates, S ~ 25 m^2/g) and various silicas (8–85 nm in diameter for primary particles, 300–600 nm in size for aggregates, S ~ 55–342 m^2/g [11,19]). We refer to previous work for preparation of initial oxides and measurement of S [20] and of core–shell type PNCs [11]. The interfacial polymer fraction (Rigid Amorphous Fraction, *RAF*) was evaluated in DSC by the deviation (missing part) of the heat capacity step of the nanocomposites (NCs) at glass transition, ΔC_p, from that of the neat polymer [1]. In BDS, on the contrary, the segmental dynamics of the polymer at the interfaces was recorded as a separate relaxation (α_{int} relaxation) [2,8,11] and *RAF* was evaluated by comparing its dielectric strength ($\Delta\varepsilon$) with that of the total segmental response (interfacial and bulk). Results by the two techniques show, in close qualitative agreement with each other, that *RAF* and the corresponding interfacial layer thickness (apparent) increase with S.

* Corresponding author.
E-mail address: pklonos@central.ntua.gr (P. Klonos).

http://dx.doi.org/10.1016/j.polymer.2015.09.021
0032-3861/

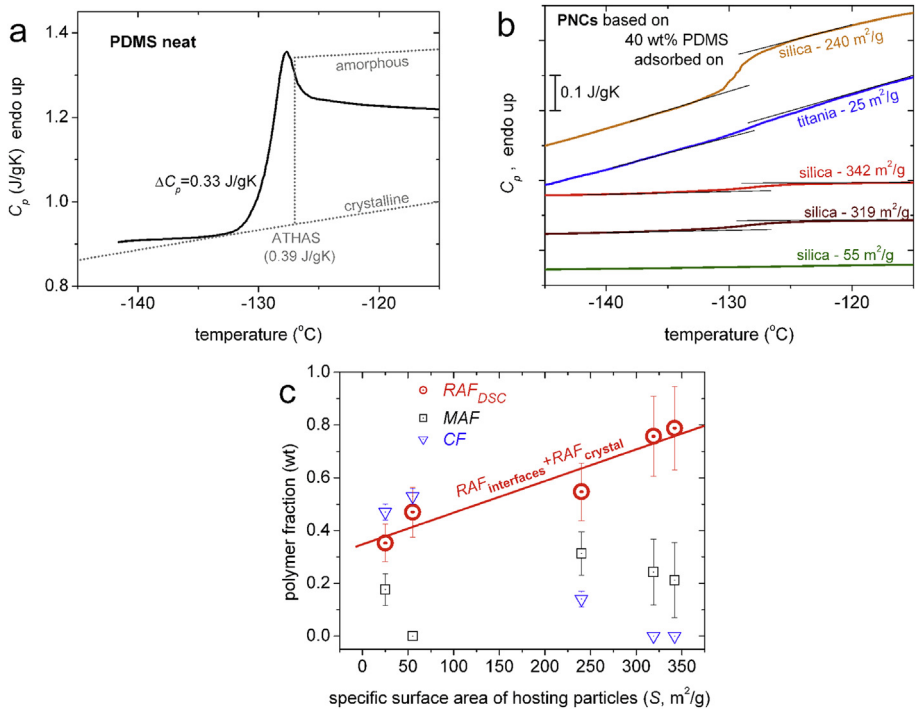

Fig. 1. (a) Comparative DSC thermograms for pure amorphous PDMS in the glass transition region. Heat capacity curves for PDMS from the ATHAS databank (Reference 24 in Ref. [1]) are also shown. (b) Comparative DSC thermograms for nanocomposite samples of 40 wt% PDMS adsorbed on silica and titania particles. The DSC curves are normalized to sample mass. (c) fractions of rigid amorphous polymer (RAF_{DSC}), mobile amorphous polymer (*MAF*) and crystalline polymer (*CF*) against specific surface area, *S*, of the hosting particles. The line in (c) is a linear fit to the RAF_{DSC} data.

Fig. 1a,b presents comparative DSC thermograms in the glass transition region for PDMS and NCs. The glass transition temperature, T_g, determined as the midpoint of the heat capacity step, ΔC_p, increases in the NCs by 1–5 K, comparing to neat amorphous PDMS (−129 °C). The heat capacity step, normalized to the same amorphous PDMS mass, $\Delta C_{p,n}$ (Eq. (3) in Ref. [8]), decreases in the NCs, due to the growth of the interfacial Rigid Amorphous Fraction, $RAF_{interfaces}$ [1]. Because of the semi–crystalline nature of PDMS, an additional Rigid Amorphous Fraction exists in close proximity to crystals, $RAF_{crystal}$ [21]. $RAF_{interfaces}$ and $RAF_{crystal}$ do not contribute to ΔC_p, forming together RAF_{DSC}. Furthermore, we employ Eq. (1) according to a '3–phase model' [1,21] and calculate RAF_{DSC}.

$$RAF_{DSC} = 1 - CF - MAF = 1 - CF - \frac{\Delta C_{p,n}(1-CF)}{\Delta C_{p,amorphous}^{PDMS}} \quad (1)$$

CF in Eq. (1) is the degree of crystallinity (obtained from the crystallization enthalpy [8] (Fig. 1c), *MAF* is the mobile amorphous polymer fraction which contributes to glass transition, and $\Delta C_{p,amorphous}^{PDMS}$ is the heat capacity change at glass transition for fully amorphous PDMS (0.33 J/gK from fast cooling measurements, Fig. 1a). In Fig. 1c we follow that RAF_{DSC} increases with *S* almost linearly, varying between 0.35 wt (titania, *S* ~25 m^2/g) and 0.79 wt (silica of *S* ~342 m^2/g).

BDS results recorded isothermally (details in Ref. [11]) have been replotted in Fig. 2a as isochronal imaginary part of dielectric permittivity $\varepsilon''(T)$ plots to facilitate direct comparison with the DSC thermograms of Fig. 1a,b. A relative to DSC high frequency of 3.1 kHz was selected to suppress effects of conductivity [22]. Fig. 2b shows effects imposed by polymer adsorption on the real part of dielectric permittivity, ε', of initial oxides at −150 °C (below T_g), where the dipoles related to polymer segmental dynamics do not contribute to dielectric response (immobile polymer chains). Additionally, BDS results were analyzed by fitting the Havriliak–Negami (HN) equation [11,22]

$$\varepsilon^*(f) = \frac{\Delta\varepsilon}{(1+(if/f_0)^{\alpha_{HN}})^{\beta_{HN}}} \quad (2)$$

to the experimental data in order to evaluate the time scale (temperature dependence of the frequency maxima) (Fig. 3a) and the dielectric strength, $\Delta\varepsilon$, (Fig. 3b) of the various relaxations [22]. In Eq. (2), f_0 is a characteristic frequency related to the frequency of maximum dielectric loss, and α_{HN} and β_{HN} are the shape parameters of the relaxation. One HN term of the type (2) for each of the relaxations (namely α_{bulk}, α_{int}, and S_{OH}, the local relaxation of the –OH groups on the surface of the particles [23]) was fitted to the experimental data at each temperature and the fitting parameters were determined, compare Refs. [2,11] for details.

The bulk segmental relaxation (α_{bulk}) consists of two contributions, arising from extended amorphous regions and from polymer chains restricted between condensed crystalline regions, respectively, more clearly discerned for neat PDMS in Fig. 2a. In the NCs one of the two contributions dominates depending on the degree of crystallinity. α_{bulk} becomes gradually weaker with the increasing of *S* (Fig. 3b). The S_{OH} relaxation dominates the response of initial nanooxides (not shown) [11] and is present here in the NCs of high specific surface area (Fig. 3).

The most interesting results come from the slower α_{int} process (Figs. 2a and 3a), which monitors the segmental dynamics in the interfacial polymer layer [2,8,11]. With *S* increasing, α_{int} becomes faster (Fig. 3a), stronger (Fig. 3b), and more cooperative (higher fragility index *m* in Fig. 4, details of calculation in Ref. [11]).

By employing a model analog to the one used previously for DSC (Eq. (1)) we calculate the interfacial PDMS fraction in the NCs, $RAF_{interfaces}$, according to the following equation.

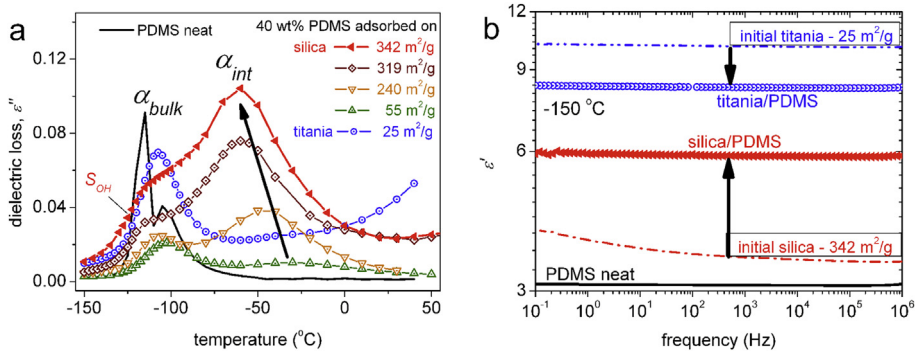

Fig. 2. (a) Comparative isochronal plots of the imaginary part of dielectric permittivity (dielectric loss), ε'', at 3.1 kHz for 40 wt% PDMS adsorbed in silica and titania and for pure PDMS. (b) shows selected results for the real part of dielectric permittivity, ε', at −150 °C against frequency for the initial components (titania, silica and PDMS) and the respective composites.

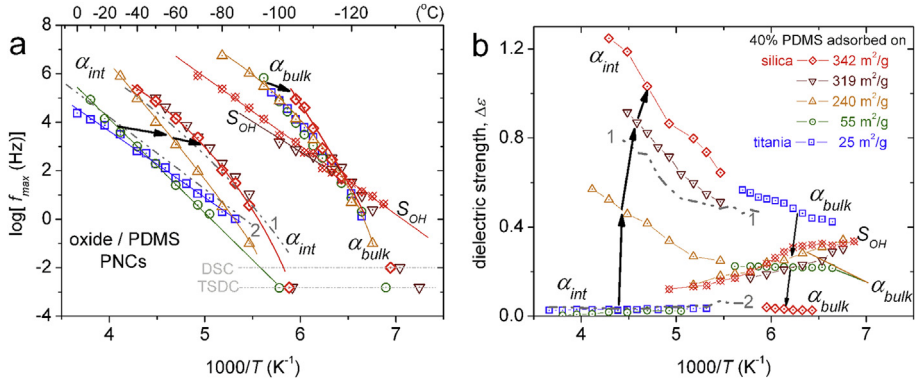

Fig. 3. (a) Arrhenius plots and (b) dielectric strength vs reciprocal temperature for the segmental relaxations of bulk (α_{bulk}) and interfacial polymer (α_{int}) and for the local relaxation of the −OH groups on the surface of the particles (S_{OH}) for the studied PNCs (description in (b)). The lines in (a) are fittings of the VTFH and Arrhenius equations [2]. The lines (1), (2) in both (a) and (b) correspond to the interfacial relaxation in conventional (1) PDMS/silica and (2) PDMS/titania nanocomposites [8]. Included in (a) are DSC and TSDC data [11]. The arrows mark changes imposed by increasing of S.

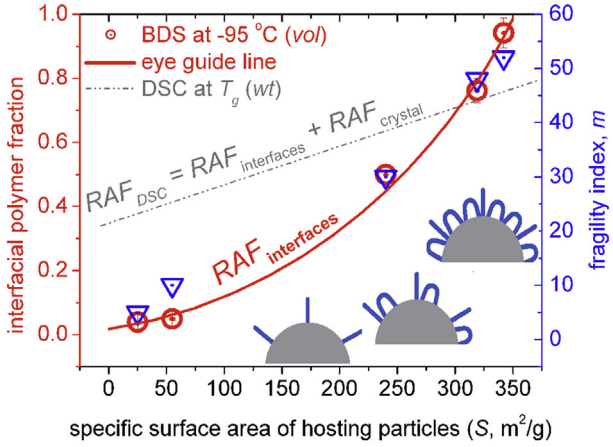

Fig. 4. (Left axis, cycles) interfacial polymer fraction ($RAF_{interfaces}$) and (right axis, triangles) fragility index, m, of the interfacial relaxation (α_{int}) against specific surface area, S, obtained by BDS at −95 °C. RAF_{DSC} (interfacial and around crystals) at T_g obtained by DSC is also shown (dash–dotted line, values refer to the left axis). The insets show simplified models for the conformations of polymer chains on the surface of nano-oxides for the different S.

$$RAF_{interfaces} = \frac{\Delta\varepsilon_{\alpha,\mathrm{int}}(1 - CF)}{\Delta\varepsilon_{\alpha,bulk} + \Delta\varepsilon_{\alpha,\mathrm{int}}} \quad (3)$$

From the methodological point of view, Eq. (3) involves the total dielectric response of the segmental relaxations for each sample. Thus, we may assume that any systematic errors in the calculations and the comparison between different samples, arising from possible differences in polarizability of PDMS chains in the different fractions [24], are reduced by this calculation method. The suitability of Eq. (3) for calculating interfacial polymer fraction has been confirmed in NCs based on silica and various polymers of both amorphous [9,10,25] and semi-crystalline type [8,19]. Results for $RAF_{interfaces}$ are shown in Fig. 4, for −95 °C ($\Delta\varepsilon$ changes with temperature, Fig. 3b). They reveal that, next to enhanced dynamics and cooperativity, $RAF_{interfaces}$ increases systematically with S, in qualitative agreement with DSC, despite *in principle* different methods of measurement and calculation [5].

In our recent work on similar *core–shell* systems [11,19] we have discussed results for the interfacial α_{int} process in terms of the formation of two types of segment conformations at interfaces, namely (a) extended tails with bulk–like density but reduced mobility, and (b) loop–like chain segments with multiple contact points with the silica surface resulting in increased density and cooperativity (schemes in Fig. 4) [17]. Obviously, both types of segments are characterized by increased orientation (order) and polarizability, as compared to segments in the bulk, which explains the increased dielectric response in the NCs beyond additivity (Fig. 2b). The loops/tails ratio should increase with increasing S as depicted in Fig. 4. This dependence is also at the origin of an explanation for the increase/decrease of $\Delta\varepsilon$ of α_{int} relaxation with temperature, for samples of respectively high/low interfacial

polymer fraction in Fig. 3b, details in Refs. [11,17]. In addition, increase in nanometric surface roughness in the present work leads to increased number of contact points and, therefore, gradually denser interfacial layer [17]. This implies reduction of the cooperativity length ξ, thus, in the frame of Adam–Gibbs theory [26], faster and more cooperative segmental dynamics is expected, in agreement with results for α_{int} here (Figs. 3a and 4). We have recently showed [19] that surface modification of low specific surface area fumed silica (58 m^2/g) with small zirconia nanoparticles resulted in slightly increased S and in faster and more cooperative interfacial relaxation, these effects suggesting an increase of PDMS–particle contact points, in qualitative agreement with effects obtained here with S and α_{int} of the NCs. Finally, the adequacy of the model proposed above was examined, additionally, in our recent work [27] in similar systems of silica/PDMS by means of (a) surface modification of silica of initially high S (342 m^2/g) with zirconia nanoparticles resulting in strongly suppressed S and (b) thermal (crystallization) annealing, the results for interfacial polymer being in qualitative agreement with those obtained in the present study.

A term often employed for the description of the range [2,10] of polymer–filler interactions is the distance from the particles' surface, up to which the characteristics of interfacial (modified) polymer dominate, in other words, the thickness of the interfacial layer [15]. Assuming (i) constant density of PDMS in the interfacial layer and in bulk, equal to that of neat PDMS ($\rho_{PDMS} = 1.62$ g/cm^3) [8], and (ii) accessibility of the whole oxide surface area to PDMS (please note, S was determined from nitrogen adsorption–desorption measurements [20]), we estimate the *'apparent' interfacial layer thickness*, d_{int}, by the following simple equation.

$$d_{\mathrm{int}} = \frac{volume_{interfacial,PDMS}}{surface_{interfacial}} = \frac{mass_{sample} \cdot X_{PDMS} \cdot RAF_{interfacial}/\rho_{PDMS}}{mass_{sample} \cdot (1 - X_{PDMS}) \cdot S} \quad (4)$$

The results show that d_{int} increases in general with S varying between 0.37 and 1.10 nm. The relatively low absolute values, smaller than values obtained in conventional PDMS/silica NCs (~2 nm) [2,8], also smaller than the *Kuhn segment length* for PDMS (1.56 nm [28]) by a factor of 2–4, can be probably understood in terms of assumption (ii) above (apparent values). Kumar and coworkers discussed d_{int} values in relation to *Kuhn segment length*, which should be at the upper limit of d_{int} [15]. The deviation of d_{int} from the *Kuhn segment length* of PDMS may be useful for rationalizing results by Eq. (4) in the frame of assumption (ii).

In summary, BDS in combination with DSC revealed that the increase of specific surface area, S, of silica–like oxide particles results in increase of polymer–particle contact points, reflected in increased interfacial polymer fraction and, furthermore, enhanced mobility and cooperativity. In an attempt to explain the changes on the overall dielectric response (ε'', ε', $\Delta\varepsilon$), the characteristics of interfacial relaxation were interpreted in terms of bimodal conformations (tail– and loop–like) of PDMS at the oxide surfaces. The increase of d_{int} (apparent values) with S, surprising at first glance, is probably related to the reported increase of mean pore size with S [20], resulting in increased accessibility of the oxide surface to PDMS, a point worth to be followed in future work.

Acknowledgments

The authors would like to thank Prof. Vladimir M. Gun'ko from the Institute of Surface, NASU, Kiev, Ukraine, for providing the materials.

This research has been co–financed by the European Union (European Social Fund – ESF) and Greek National Funds through the Operational Program "Education and Lifelong Learning" of the National Strategic Reference Framework (NSRF) – Research Funding Programs: Heracleitus II. Investing in knowledge society through the European Social Fund (P.K. and P.P.) and Research Funding Program: Aristeia (A.K. and P.P.).

References

[1] A. Wurm, M. Ismail, B. Kretzschmar, D. Pospiech, C. Schick, Macromolecules 43 (2010) 1480–1487, http://dx.doi.org/10.1021/ma902175r.
[2] D. Fragiadakis, P. Pissis, J. Non Cryst Solids 353 (2007) 4344–4352, http://dx.doi.org/10.1016/j.jnoncrysol.2007.05.183.
[3] P. Akcora, H. Liu, S.K. Kumar, J. Moll, Y. Ki, B.C. Benicewicz, L.S. Schadler, D. Acehan, A.Z. Panagiotopoulos, V. Pryamitsyn, V. Ganesan, J. Ilavsky, R. Thiyagarajan, R.H. Colby, J.F. Douglas, Nat. Mater. 8 (2009) 354–359, http://dx.doi.org/10.1038/nmat2404.
[4] V.M. Boucher, D. Cangialosi, A. Alegría, J. Colmenero, J. Gonzalez–Irun, L.M. Liz–Marzan, Soft Matter 6 (2010) 3306–3317, http://dx.doi.org/10.1039/c001656j.
[5] H. Eslami, M. Rahimi, F. Müller–Plathe, Macromolecules 46 (2013) 8680–8692, http://dx.doi.org/10.1021/ma401443v.
[6] G.G. Vogiatzis, D.N. Theodorou, Macromolecules 46 (2013) 4670–4683, http://dx.doi.org/10.1021/ma400107q.
[7] A.N. Rissanou, V. Harmandaris, Soft Matter 10 (2014) 2876–2888, http://dx.doi.org/10.1039/c3sm52688g.
[8] P. Klonos, A. Panagopoulou, L. Bokobza, A. Kyritsis, V. Peoglos, P. Pissis, Polymer 51 (2010) 5490–5499, http://dx.doi.org/10.1016/j.polymer.2010.09.054.
[9] M. Füllbrandt, P.J. Purohit, A. Schönhals, Macromolecules 46 (2013) 4626–4632, http://dx.doi.org/10.1021/ma400461p.
[10] A.P. Holt, P.J. Griffin, V. Bocharova, A.L. Agapov, A.E. Imel, M.D. Dadmun, J.R. Sangoro, A.P. Sokolov, Macromolecules 47 (2014) 1837–1843, http://dx.doi.org/10.1021/ma5000317.
[11] P. Klonos, I.Y. Sulym, M.V. Borysenko, V.M. Gun'ko, S. Kripotou, A. Kyritsis, P. Pissis, Polymer 58 (2015) 9–21, http://dx.doi.org/10.1016/j.polymer.2014.12.037.
[12] M.V. Galaburda, P. Klonos, V.M. Gun'ko, V.M. Bogatyrov, M.V. Borysenko, P. Pissis, Appl. Surf. Sci. 305 (2014) 67–76, http://dx.doi.org/10.1016/j.apsusc.2014.02.162.
[13] D.F. Schmidt, E.P. Giannelis, Chem. Mater. 22 (2010) 167–174, http://dx.doi.org/10.1021/cm9026978.
[14] S.E. Harton, S.K. Kumar, H. Yang, T. Koga, K. Hicks, H.K. Lee, J. Mijovic, M. Liu, R.S. Vallery, D.W. Gidley, Macromolecules 43 (2010) 3415–3421, http://dx.doi.org/10.1021/ma902484d.
[15] S. Gong, Q. Chen, J.F. Moll, S.K. Kumar, R.H. Colby, ACS Macro Lett. 3 (2014) 773–777, http://dx.doi.org/10.1021/mz500252f.
[16] L.T. Lee, O. Guiselin, A. Lapp, B. Farnoux, Phys. Rev. Lett. 67 (1991) 20, http://dx.doi.org/10.1103/PhysRevLett.67.2838.
[17] P. Gin, N. Jiang, C. Liang, T. Taniguchi, B. Akgun, S.K. Satija, M.K. Endoh, T. Koga, Phys. Rev. Lett. 109 (2012) 265501, http://dx.doi.org/10.1103/PhysRevLett.109.265501.
[18] C. Rotella, S. Napolitano, S. Vandendriessche, V.K. Valev, T. Verbiest, M. Larkowska, S. Kucharski, M. Wübbenhorst, Langmuir 27 (2011) 13533, http://dx.doi.org/10.1021/la2027779.
[19] P. Klonos, I.Y. Sulym, K. Kyriakos, I. Vangelidis, S. Zidropoulos, D. Sternik, M.V. Borysenko, A. Kyritsis, A. Deryło–Marczewska, V.M. Gun'ko, P. Pissis, Polymer 68 (2015) 158–167, http://dx.doi.org/10.1016/j.polymer.2015.05.017.
[20] I.Y. Sulim, M.V. Borysenko, O.M. Korduban, V.M. Gun'ko, Appl. Surf. Sci. 255 (2009) 7818–7824, http://dx.doi.org/10.1016/j.apsusc.2009.04.185.
[21] J. Dobbertin, A. Hensel, C. Schick, J. Therm. Anal. Calorim. 47 (1996) 1027–1040, http://dx.doi.org/10.1007/BF01979446.
[22] F. Kremer, A. Schoenhals (Eds.), Broadband Dielectric Spectroscopy, Springer, Berlin, 2002.
[23] J.J. Fontanella, M.C. Wintersgill, C.A. Edmondson, J.F. Lomax, J. Phys. D Appl. Phys. 42 (2009) 042003, http://dx.doi.org/10.1088/0022-3727/42/4/042003.
[24] S. Capponi, S. Napolitano, M. Wübbenhorst, Nat. Commun. 3 (2012) 1233, http://dx.doi.org/10.1038/ncomms2228.
[25] D. Fragiadakis, L. Bokobza, P. Pissis, Polymer 52 (2011) 3175–3182, http://dx.doi.org/10.1016/j.polymer.2011.04.045.
[26] G. Adam, J.H. Gibbs, J. Chem. Phys. 43 (1965) 139–146, http://dx.doi.org/10.1063/1.1696442.
[27] P. Klonos, A. Kyritsis, P. Pissis, Eur. Polym. J. 70 (2015) 342–359, http://dx.doi.org/10.1016/j.eurpolymj.2015.07.038.
[28] N. Gilra, C. Cohen, R.M. Briber, B.J. Bauer, R.C. Hedden, A.Z. Panagiotopoulos, Macromolecules 34 (2001) 7773–7782, http://dx.doi.org/10.1021/ma010018+.